Journal of Solid State Chemistry 185 (2012) 37–41

Contents lists available at SciVerse ScienceDirect

Journal of Solid State Chemistry

journal homepage: www.elsevier.com/locate/jssc

Two coordination polymers of manganese(II) isophthalate and their preparation, structures, and magnetic properties

Jinxi Chen [a,*], Jingjing Wang [a], Masaaki Ohba [b]

[a] School of Chemistry and Chemical Engineering, Southeast University, Nanjing 211189, PR China
[b] Department of Chemistry, Faculty of Science, Kyushu University, Fukuoka, Japan

ARTICLE INFO

Article history:
Received 10 August 2011
Received in revised form
18 October 2011
Accepted 30 October 2011
Available online 9 November 2011

Keywords:
Coordination polymers
Manganese
Isophthalate
Magnetic properties

ABSTRACT

Two manganese coordination polymers, $[Mn_2(ip)_2(dmf)]\cdot dmf$ (**1**) and $[Mn_4(ip)_4(dmf)_6]\cdot 2dmf$ (**2**) (ip=isophthalate; dmf=N,N-dimethylformamide), have been synthesized and characterized. X-ray crystal structural data reveal that compound **1** crystallizes in triclinic space group $P-1$, $a=9.716(3)$ Å, $b=12.193(3)$ Å, $c=12.576(3)$ Å, $\alpha=62.19(2)^\circ$, $\beta=66.423(17)^\circ$, $\gamma=72.72(2)^\circ$, $Z=2$, while compound **2** crystallizes in monoclinic space group Cc, $a=19.80(3)$ Å, $b=20.20(2)$ Å, $c=18.01(3)$ Å, $\beta=108.40(4)^\circ$, $Z=4$. Variable-temperature magnetic susceptibilities of compounds **1** and **2** exhibit overall weak antiferromagnetic coupling between the adjacent Mn(II) ions.

1. Introduction

Porous coordination polymers (PCPs) or metal organic frameworks (MOFs) have attracted extensive interests in the past two decades because of their intriguing structural diversity and potential applications as functional materials in gas storage, separation processes, magnetism, drug delivery, catalysis, and chemical sensing [1–6]. This class of materials can be easily obtained through self-assembly of multidentate organic ligands as linkers and metal ions or metal clusters as connecting nodes. A great number of PCPs prepared using carboxylic acids with two or more carboxylate arms have been reported in this burgeoning field [7], and several of them (such as HKUST-1 and MIL-53) are available commercially. As part of ongoing research work on the PCPs of polycarboxylates in our group, several metal carboxylates with interesting properties have been successfully prepared [8]. Such interesting results have intrigued us to continue to explore the construction of PCPs based on other polycarboxylates, especially those possessing magnetic properties. A typical aromatic polycarboxylate ligand, isophthalic acid (H_2ip) has been widely used to construct PCPs. It features two excellent characteristics as follows: (i) it has two carboxyl groups with a 120° angle between them, and thus can present versatile coordination modes and yield predetermined networks, and (ii) its carboxylate and phenyl groups can function as mediator for transmitting exchange interaction between paramagnetic metal centers. On the other hand, among the most commonly used transition metal elements in the realm of PCPs, manganese is attracting considerable attention because of its ability to function as a binder for constructing the coordination framework and as a progenitor of novel magnetic molecular materials. In the current paper, we report two manganese isophthalates, $[Mn_2(ip)_2(dmf)]\cdot dmf$ (**1**) and $[Mn_4(ip)_4(dmf)_6]\cdot 2dmf$ (**2**) (ip=isophthalate), which are solvothermally and liquid–liquid diffusion synthesized, respectively. Crystal structural data reveal that compound **1** adopts a three-dimensional structure containing $(MnO)_n$ inorganic chains, while compound **2** adopts a two-dimensional layered feature consisting of dimeric Mn_2 building block units. Variable-temperature magnetic susceptibility measurements exhibit weak antiferromagnetic interactions between the Mn(II) ions in both compounds.

2. Experimental

2.1. Materials and general methods

All solvents and reagents were obtained from Aldrich or TCI and used without further purification. C, H, and N elemental microanalysis data were obtained using a Vario EL elemental analyzer. FT-IR spectra (KBr) were recorded in the range of 4000–400 cm^{-1} on a Bruker IFS 66v/S Fourier-transform infrared spectrometer.

2.2. Syntheses

2.2.1. Synthesis of $[Mn_2(ip)_2(dmf)]\cdot dmf$ (**1**)

H_2ip (1.00 mmol, 0.166 g), $MnCl_2\cdot 4H_2O$ (1.00 mmol, 0.198 g), and dmf (8.0 mL) were successively added to a 23 mL Teflon

* Corresponding author. Fax: +86 25 52090618.
E-mail address: chenjinxi@seu.edu.cn (J. Chen).

0022-4596/$ - see front matter © 2011 Elsevier Inc. All rights reserved.
doi:10.1016/j.jssc.2011.10.051

autoclave, and the formed mixture was then heated to 150 °C in 2 h and kept at this temperature for 3 days. After heating, it was allowed to cool to room temperature at a rate of 5 °C per hour. A product in light yellow platelets was separated through filtration with yield of 75% based on the ligand. Anal. Calcd for $C_{22}H_{22}Mn_2N_2O_{10}$ (%) C 45.18, N 4.79, H 3.77. Found: C 44.83, N 4.58, H 4.01. IR data (KBr, cm^{-1}): 3064w, 2939m, 2814w, 1669s, 1614m, 1492m, 1396s, 1259m, 1195m, 978w, and 930m.

2.2.2. Synthesis of $[Mn_4(ip)_4(dmf)_6]\cdot 2dmf$ (**2**)

Compound **2** was prepared through liquid–liquid diffusion at room temperature. H_2ip (1.00 mmol, 0.166 g) and $MnCl_2\cdot 4H_2O$ (1.00 mmol, 0.198 g) were dissolved in dmf (15.0 mL), into which a solution mixture of triethylamine (0.2 mL) and dmf (2.0 mL) was allowed to diffuse slowly. After 2 weeks, compound **2** was isolated as light yellow needle-like crystals with yield of 58% based on ligand from the reaction mixture. Anal. Calcd for $C_{56}H_{72}Mn_4N_8O_{24}$ (%): C 46.00, N 7.67, H 4.93. Found: C 45.66, N 7.44, H 5.18. IR data (KBr, cm^{-1}) 3064w, 2935m, 2810w, 1671s, 1605m, 1496m, 1396s, 1259m, 1124m, 978w, and 934m.

2.3. Crystallographic data collection and structures

X-ray diffraction measurements for compounds **1** and **2** were carried out on a Rigaku Mercury CCD in the θ range of 3.19–27.48° for **1** and 2.02–30.27° for **2** at 293 K, using graphite-monochromated Mo $K\alpha$ radiation (λ=0.7107 Å). Their structures were solved with direct methods using SIR 97. All compounds were expanded using Fourier techniques. All non-hydrogen atoms were refined anisotropically with the full-matrix least-squares method on F^2. The hydrogen atoms were generated geometrically. All calculations were carried out on a SGI workstation using the teXsan crystallographic software package of Molecular Structure Corporation. The crystal parameters, data collection, and refinement results for compounds **1** and **2** are summarized in Table 1. Selected bond lengths and angles are listed in Table 2.

2.4. Magnetic susceptibility measurements

Direct current (dc) magnetic measurements for powder crystalline samples of **1** and **2** were made on a Quantum Design MPMS-XL SQUID magnetometer in the temperature range of 2–300 K and with an applied field of 10 kOe. Samples were packed in a gelatin capsule for the measurements. Magnetic susceptibility of the gelatin capsule was subtracted from the raw data in each sample. Diamagnetic susceptibility of the sample was corrected with the conventional Pascal method.

3. Results and discussion

3.1. Crystal structures

Single-crystal X-ray analysis indicates that complex **1** adopts a three-dimensional (3D) porous structure consisting of five-coordinate and six-coordinate manganese(II) atoms. As shown in Fig. 1, the asymmetric unit comprises of two halves of an octahedrally coordinated MnO_6 unit that has crystallographically imposed inversion, one five-coordinate MnO_5 unit, one μ_2-bridging dmf molecule, two isophthalate ligands, and one uncoordinated free dmf molecule. The trigonal–bipyramidal geometry of $Mn(1)O_5$ unit has one dmf O donor (O(9)) and four carboxyl O donors (O(1), $O(3)^{\#2}$, O(5) and $O(8)^{\#1}$) from two different ip moieties (symmetry operations: #1: $-x+2$, $-y+1$, $-z+1$; #2: $x-1$, y, z). The $Mn(2)O_6$ unit is composed of six carboxylate O donors (O(2), $O(2)^{\#3}$, $O(4)^{\#2}$, $O(4)^{\#4}$, O(5) and $O(5)^{\#3}$), while the $Mn(3)O_6$ unit consists of four carboxylate O donors (O(6), $O(6)^{\#6}$, $O(7)^{\#1}$ and $O(7)^{\#5}$) and two dmf O donors (O(9) and $O(9)^{\#6}$) (symmetry operations: #3: $-x+2$, $-y$, $-z+2$; #4: $-x+3$, $-y$, $-z+2$; #5: x, y, $z+1$; #6: $-x+2$, $-y+1$, $-z+2$). The O(9) and O(5) donors are bridged between Mn(1) and Mn(3), and Mn(1) and Mn(2), respectively, in a μ_2–O fashion. In the lattice, infinite $(MnO)_n$ inorganic chains run parallel to the b axis and are interconnected by the organic ligands into a 3D structure to form

Table 1
Crystal data and structure refinement for compounds **1** and **2**.

	1	**2**
Empirical formula	$C_{22}H_{22}Mn_2N_2O_{10}$	$C_{56}H_{72}Mn_4N_8O_{24}$
Formula weight	584.30	1460.98
Crystal size (mm)	0.2 × 0.2 × 0.3	0.25 × 0.25 × 0.4
Crystal system	Triclinic	Monoclinic
Space group	$P-1$	Cc
a (Å)	9.716(3)	19.80(3)
b (Å)	12.193(3)	20.20(2)
c (Å)	12.576(3)	18.01(3)
α (deg.)	62.19(2)	90
β (deg.)	66.423(17)	108.40(4)
γ (deg.)	72.72(2)	90
V (Å^3)	1196.4(5)	6839(16)
Z	2	4
D(calcd) (g m^{-3})	1.622	1.419
μ (mm^{-1})	1.115	0.802
θ range for data collection (deg.)	3.19–27.48	2.02–30.27
Reflections collected/unique	9391/5211 [R(int)=0.0288]	25,162/15,791 [R(int)=0.0230]
Data/restraints/parameters	5211/0/328	15791/2/ 829
Goodness-of-fit on F^2	1.089	1.013
Final R indices [I > 2σ (I)]	R_1,=0.0462[a], wR_2=0.1329[b]	R_1,=0.0405[a], wR_2=0.1056[b]
R indices (all data)	R_1,=0.0492[a], wR_2=0.1372[b]	R_1,=0.0444[a], wR_2=0.1116[b]
Largest diff. peak and hole (Å^{-3})	1.918 and −0.735e	0.984 and −0.488e

[a] $R=\Sigma||F_0|-|F_c||/\Sigma|F_0|$.

[b] wR $(F^2)=[\Sigma w(F_0^2-F_c^2)^2/\Sigma w(F_0^2)^2]^{1/2}$.Weighting: $w=1/[\sigma^2(F_o^2)+(0.0573P)^2+1.29P]$, where $P=(_{\rm Max}(F_o^2, 0)+2F_c^2)/3$ for **1**. $w=1/[\sigma^2(F_o^2)+(0.0647P)^2+0.00P]$, where $P=(_{\rm Max}(F_o^2, 0)+2F_c^2)/3$ for **2**.

Table 2
Selective bond lengths (Å) and angles (deg.) for compound **1** and **2**.

Compound **1**					
Bond lengths (Å)					
Mn(1)–O(1)	2.103(2)	Mn(1)–O(9)	2.461(2)	Mn(3)–O(6)	2.2286(19)
Mn(1)–O(3)$^{\#2}$	2.133(2)	Mn(2)–O(2)	2.0875(19)	Mn(3)–O(7)$^{\#1}$	2.1079(19)
Mn(1)–O(5)	2.1745(19)	Mn(2)–O(4)$^{\#2}$	2.141(2)	Mn(3)–O(9)	2.257(2)
Mn(1)–O(8)$^{\#1}$	2.052(2)	Mn(2)–O(5)	2.3357(19)		
Angles (deg.)					
O(1)–Mn(1)–O(3)$^{\#2}$	96.67(9)	O(2)–Mn(2)–O(2)$^{\#3}$	180.000	O(6)–Mn(3)–O(6)$^{\#6}$	180.000
O(1)–Mn(1)–O(5)	94.32(8)	O(2)–Mn(2)–O(4)$^{\#2}$	92.75(9)	O(6)–Mn(3)–O(7)$^{\#1}$	91.85(8)
O(1)–Mn(1)–O(8)$^{\#1}$	88.66(8)	O(2)–Mn(2)–O(4)$^{\#4}$	87.25(9)	O(6)–Mn(3)–O(7)$^{\#5}$	88.15(8)
O(1)–Mn(1)–O(9)	178.16(8)	O(2)–Mn(2)–O(5)	88.96(8)	O(6)–Mn(3)–O(9)	83.16(8)
O(3)$^{\#2}$–Mn(1)–O(5)	120.50(9)	O(2)–Mn(2)–O(5)$^{\#3}$	91.04(8)	O(6)–Mn(3)–O(9)$^{\#6}$	96.84(8)
O(3)$^{\#2}$–Mn(1)–O(8)$^{\#1}$	101.30(9)	O(4)$^{\#2}$–Mn(2)–O(4)$^{\#4}$	180.000	O(7)$^{\#1}$–Mn(3)–O(7)$^{\#5}$	180.000
O(3)$^{\#2}$–Mn(1)–O(9)	84.61(8)	O(4)$^{\#2}$–Mn(2)–O(5)	78.14(9)	O(7)$^{\#1}$–Mn(3)–O(9)	91.18(8)
O(5)–Mn(1)–O(8)$^{\#1}$	137.32(8)	O(4)$^{\#2}$–Mn(2)–O(5)$^{\#3}$	101.86(9)	O(7)$^{\#1}$–Mn(3)–O(9)$^{\#6}$	88.82(8)
O(5)–Mn(1)–O(9)	86.16(7)	O(5)–Mn(2)–O(5)$^{\#3}$	180.000	O(9)–Mn(3)–O(9)$^{\#6}$	180.000
O(8)$^{\#1}$–Mn(1)–O(9)	89.78(8)				
Mn(1)–O(5)–Mn(2)	102.89(7)	Mn(1)–O(9)–Mn(3)	98.52(8)		
Compound **2**					
Bond lengths (Å)					
Mn(1)–O(1)	2.137(3)	Mn(2)–O(7)	2.230(3)	Mn(3)–O(13)	2.185(3)
Mn(1)–O(2)	2.225(3)	Mn(2)–O(8)	2.243(3)	Mn(3)–O(21)$^{\#2}$	2.129(3)
Mn(1)–O(3)$^{\#1}$	2.129(3)	Mn(2)–O(16)	2.315(4)	Mn(4)–O(10)	2.089(3)
Mn(1)–O(4)	2.208(3)	Mn(2)–O(19)$^{\#1}$	2.106(3)	Mn(4)–O(14)	2.102(4)
Mn(1)–O(5)	2.166(4)	Mn(3)–O(9)	2.130(4)	Mn(4)–O(15)$^{\#2}$	2.202(3)
Mn(1)–O(22)	2.166(4)	Mn(3)–O(10)	2.206(3)	Mn(4)–O(17)$^{\#3}$	2.263(3)
Mn(2)–O(4)	2.279(3)	Mn(3)–O(11)	2.171(4)	Mn(4)–O(18)$^{\#3}$	2.285(4)
Mn(2)–O(6)	2.089(3)	Mn(3)–O(12)	2.149(4)	Mn(4)–O(20)	2.307(4)
Angles (deg.)					
O(1)–Mn(1)–O(2)	83.91(11)	O(6)–Mn(2)–O(7)	91.38(13)	O(11)–Mn(3)–O(13)	94.58(12)
O(1)–Mn(1)–O(3)$^{\#1}$	96.73(12)	O(6)–Mn(2)–O(8)	149.68(10)	O(11)–Mn(3)–O(21)$^{\#2}$	171.38(10)
O(1)–Mn(1)–O(4)	94.40(11)	O(6)–Mn(2)–O(16)	98.45(10)	O(12)–Mn(3)–O(13)	89.77(12)
O(1)–Mn(1)–O(5)	88.02(13)	O(6)–Mn(2)–O(19)$^{\#1}$	96.23(11)	O(12)–Mn(3)–O(21)$^{\#2}$	85.82(11)
O(1)–Mn(1)–O(22)	168.09(10)	O(7)–Mn(2)–O(8)	58.30(10)	O(13)–Mn(3)–O(21)$^{\#2}$	89.64(12)
O(2)–Mn(1)–O(3)$^{\#1}$	88.60(11)	O(7)–Mn(2)–O(16)	97.87(11)	O(10)–Mn(4)–O(14)	111.25(11)
O(2)–Mn(1)–O(4)	172.98(9)	O(7)–Mn(2)–O(19)$^{\#1}$	111.12(13)	O(10)–Mn(4)–O(15)$^{\#2}$	90.44(11)
O(2)–Mn(1)–O(5)	98.26(11)	O(8)–Mn(2)–O(16)	86.85(11)	O(10)–Mn(4)–O(17)$^{\#3}$	95.43(8)
O(2)–Mn(1)–O(22)	86.78(11)	O(8)–Mn(2)–O(19)$^{\#1}$	95.09(11)	O(10)–Mn(4)–O(18)$^{\#3}$	144.91(9)
O(3)$^{\#1}$–Mn(1)–O(4)	84.82(10)	O(16)–Mn(2)–O(19)$^{\#1}$	147.04(10)	O(10)–Mn(4)–O(20)	57.38(8)
O(3)$^{\#1}$–Mn(1)–O(5)	172.05(10)	O(9)–Mn(3)–O(10)	91.05(11)	O(14)–Mn(4)–O(15)$^{\#2}$	97.22(10)
O(3)$^{\#1}$–Mn(1)–O(22)	90.42(12)	O(9)–Mn(3)–O(11)	89.66(12)	O(14)–Mn(4)–O(17)$^{\#3}$	151.69(9)
O(4)–Mn(1)–O(5)	88.47(10)	O(9)–Mn(3)–O(12)	175.57(11)	O(14)–Mn(4)–O(18)$^{\#3}$	93.19(13)
O(4)–Mn(1)–O(22)	95.71(10)	O(9)–Mn(3)–O(13)	88.03(12)	O(14)–Mn(4)–O(20)	98.47(10)
O(5)–Mn(1)–O(22)	86.00(13)	O(9)–Mn(3)–O(21) $^{\#2}$	98.00(11)	O(15)$^{\#2}$–Mn(4)–O(17)$^{\#3}$	91.66(9)
O(4)–Mn(2)–O(6)	108.40(11)	O(10)–Mn(3)–O(11)	91.67(11)	O(15)$^{\#2}$–Mn(4)–O(18)$^{\#3}$	111.75(10)
O(4)–Mn(2)–O(7)	149.43(9)	O(10)–Mn(3)–O(12)	91.56(10)	O(15)$^{\#2}$–Mn(4)–O(20)	147.55(11)
O(4)–Mn(2)–O(8)	99.59(9)	O(10)–Mn(3)–O(13)	173.67(9)	O(17)$^{\#3}$–Mn(4)–O(18)$^{\#3}$	58.63(9)
O(4)–Mn(2)–O(16)	57.19(11)	O(10)–Mn(3)–O(21) $^{\#2}$	84.28(11)	O(17)$^{\#3}$–Mn(4)–O(20)	87.79(9)
O(4)–Mn(2)–O(19)$^{\#1}$	90.18(14)	O(11)–Mn(3)–O(12)	86.69(12)	O(18)$^{\#3}$–Mn(4)–O(20)	95.54(11)
Mn(1)–O(4)–Mn(2)	105.39(9)	Mn(3)–O(10)–Mn(4)	105.16(9)		

Symmetry transformations used to generate equivalent atoms: #1, $-x+2$, $-y+1$, $-z+1$; #2, $x-1$, y, z; #3, $-x+2$, $-y$, $-z+2$; #4, $-x+3$, $-y$, $-z+2$; #5, x, y, $z+1$; #6, $-x+2$, $-y+1$, $-z+2$ for **1**; #1, x, $-y+1$, $z-1/2$; #2, x, $-y$, $z+1/2$; #3, x, $y-1$, z for **2**.

an open 1D channels (Fig. 2). According to Cheetham's classification, complex **1** is herein referred to as I^1O^2 (I=inorganic; O=organic) [9]. The free space accommodates one dmf molecule per formula unit. The void volume that may be generated after the removal of the coordinating dmf molecules is 23.6% (282.0 Å^3 out of the 1196.4 Å^3 unit cell volume) of the total volume as estimated by PLATON [10]. In spite of the porosity, the adsorption isotherm of N_2 showed only surface adsorption at 77 K.

The asymmetric unit of complex **2** contains four octahedrally coordinated MnO_6 units together with four isophthalate ligands, six coordinated dmf molecules, and two uncoordinated dmf molecules (Fig. 3). Both Mn(1)O_6 and Mn(3)O_6 units have three dmf O donors (O(2), O(5) and O(22) for Mn(1), O(11), O(12) and O(13) for Mn(3)) and three carboxyl O donors (O(1), O(3)$^{\#1}$ and O(4) for Mn(1), O(9), O(10) and O(21)$^{\#2}$ for Mn(3)) from two different ip moieties, while Mn(2)O_6 and Mn(4)O_6 units have six carboxyl O donors from four different ip moieties (O(4), O(6), O(7), O(8), O(16) and O(19)$^{\#1}$ for Mn(2), O(10), O(14), O(15)$^{\#2}$, O(17)$^{\#3}$, O(18)$^{\#3}$ and O(20) for Mn(4)) (symmetry operations: #1: x, $-y+1$, $z-1/2$; #2: x, $-y$, $z+1/2$; #3: x, $y-1$, z). Mn(1) and Mn(2), also Mn(3) and Mn(4), are bridged between two carboxylate groups in the combination of *syn–syn* bidentate and monodentate μ_2–O bridging modes, and the dimer units are linked by ip moieties with nearest interdimer separation of 8.175 Å. The crosslinking of the MnO_6 units via the benzene rings results in a 2D layered structure (Fig. 4). Complex 2 would be a (I^0O^2) system.

3.2. Magnetic properties

The magnetic behaviors of compounds **1** and **2**, shown in Figs. 5 and 6, respectively, are characterized by $\chi_M T$ and χ_M in function of T. Magnetic measurements were carried out on powdered samples of **1** and **2** under an applied field of 10 kOe in the temperature range of 2–300 K. The $\chi_M T$ value is

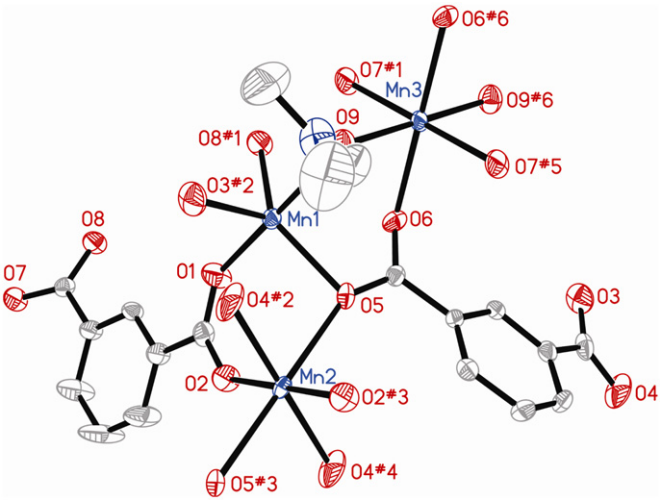

Fig. 1. View of the coordination environments of the Mn atoms in compound **1**. Hydrogen atoms and guest dmf molecules are omitted for clarity. Symmetry codes: #1, $-x+2$, $-y+1$, $-z+1$; #2, $x-1$, y, z; #3, $-x+2$, $-y$, $-z+2$; #4, $-x+3$, $-y$, $-z+2$; #5, x, y, $z+1$; #6, $-x+2$, $-y+1$, $-z+2$.

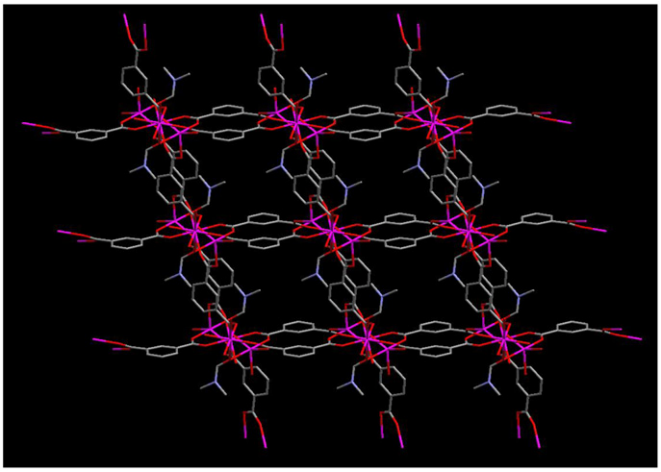

Fig. 2. View of the 1-D channels along the crystallographic *b* axis in compound **1.** Guest dmf molecules are omitted for clarity.

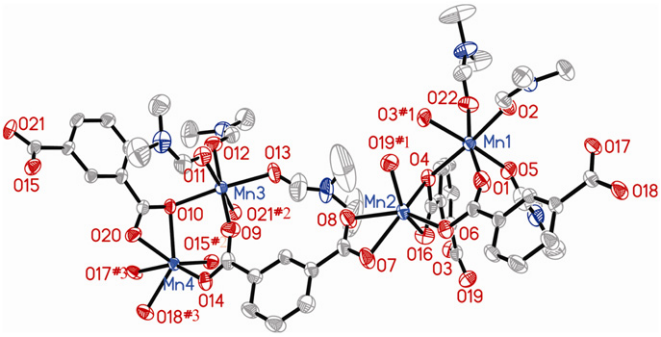

Fig. 3. View of the coordination environments of the Mn atoms in compound **2**. Hydrogen atoms and guest dmf molecules are omitted for clarity. Symmetry codes: #1, x, $-y+1$, $z-1/2$; #2, x, $-y$, $z+1/2$; #3, x, $y-1$, z.

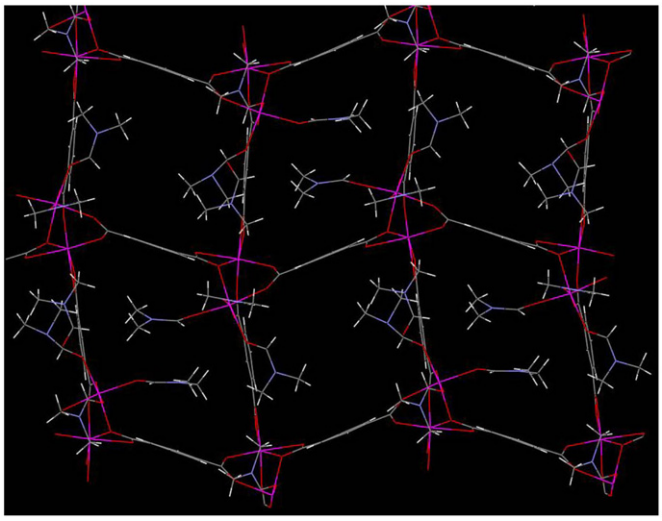

Fig. 4. View of the 2-D layered structure in compound **2**. Guest dmf molecules are omitted for clarity.

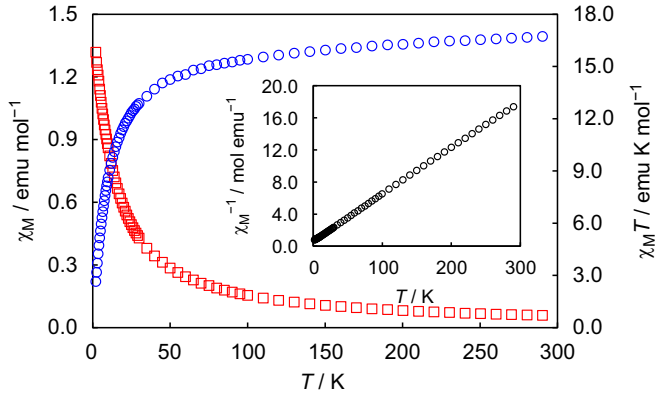

Fig. 5. Temperature dependences of χ_M (□) and $\chi_M T$ (○) for compound **1**. (Inset: χ_M^{-1} vs. T plot).

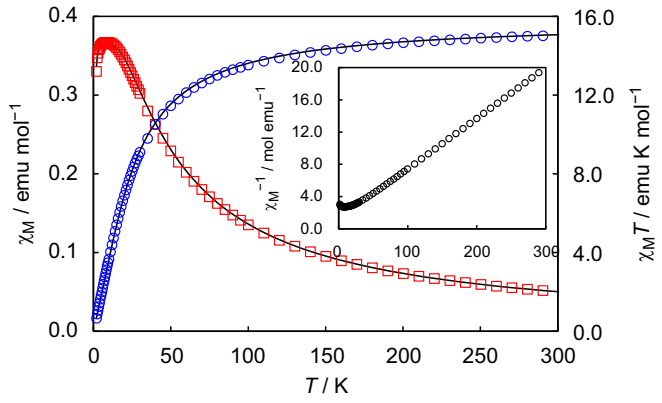

Fig. 6. Temperature dependences of χ_M (□) and $\chi_M T$ (○) for compound **2**. The solid lines represent the theoretical curve based on a dimer-of-dimers model using the parameters, $J=-1.68$ cm^{-1}, $g=1.93$ and $\rho=0.018$. (Inset: χ_M^{-1} vs. T plot).

16.78 emu kmol^{-1} at 300 K for compound **1**. As the temperature decreases, the χ_M product increases, whereas the $\chi_M T$ product decreases continuously to a minimum value of 2.64 emu kmol^{-1} at 2 K. It is linear above 20 K in the $1/\chi_M$ vs. T plot of **1**, where the Curie–Weiss law governs with $C=17.18$ emu kmol^{-1} and $\theta=-10.4$ K. The negative value of θ and an initial decrease in $\chi_M T$ should be attributed to the overall antiferromagnetic coupling between the Mn(II) ions in compound **1**. The magnetic behavior of **1** could not be analyzed theoretically because of its complicate bridging structure including *syn–syn*, *ant–anti* and *syn–anti* types of carboxylate bridges and μ_2–O bridge. Similarly, the $\chi_M T$ value for compound **2** is 15.0 emu kmol^{-1} at 300 K. With

decreasing temperature, the χ_M vs. T curve shows a peak at 9 K, while the $\chi_M T$ product decreases continuously to a minimum value of 0.68 emu kmol^{-1} at 2 K. The $1/\chi_M$ vs. T plot of **2** stays linear above 30 K and is subject to the Curie–Weiss law with $C=17.06$ emu kmol^{-1} and $\theta=-32.7$ K. The negative value of θ and an initial decrease in $\chi_M T$ should also be attributed to the overall antiferromagnetic coupling between the Mn(II) ions of compound **2**. The magnetic behavior of **2** could be well analyzed using a dimer-of-dimers model for $S=(5/2+5/2)2$. Because the bridging structures of Mn(1)Mn(2) and Mn(3)Mn(4) dinuclear units are essentially the same, the spin Hamiltonian for the system is given by $\boldsymbol{H}=-2J(S_1S_2+S_3S_4)$, where J is the exchange interaction in the dinuclear units. Magnetic analysis was carried out using the following equation:

$$\chi_M=\frac{4Ng^2\beta^2}{k(T-\theta)}\left\{\frac{55x^{30}+30x^{20}+14x^{12}+5x^6+x^2}{11x^{30}+9x^{20}+7x^{12}+5x^6+3x^2+1}(1-\rho)+\frac{35}{12}\rho\right\}$$

with $x=\exp(J/kT)$. In this equation, ρ is the fraction of Mn(II) paramagnetic impurity, θ is the correction term including inter-dimer interaction, and the remaining symbols have their usual physical meanings. As shown in Fig. 6, the magnetic behavior of **2** is well simulated with the following parameters, $J=-1.68$ cm^{-1}, $g=1.93$, $\rho=0.018$, and $\theta=0.00$ K. Although the g value is slightly small, the simulation suggests that a weak intra-dimer antiferromagnetic interaction operates between Mn(II) ions and the dimer units are magnetically independent of each other.

4. Conclusions

We have successfully and selectively synthesized two coordination polymers of manganese isophthalate, namely, $[Mn_2(ip)_2(dmf)]\cdot dmf$ (**1**) and $[Mn_4(ip)_4(dmf)_6]\cdot 2dmf$ (**2**) with solvothermal or liquid–liquid diffusion methods. X-ray crystallographic studies reveal these compounds **1** and **2** form a 3D framework with 1D channel and a 2D layered structure, respectively. Variable-temperature magnetic susceptibility measurements exhibit overall weak antiferromagnetic interactions between the Mn(II) ions in both compounds.

Supporting information available

X-ray Crystallographic data for compounds **1** and **2** in CIF form. CCDC 837897 and 837898 contain the crystallographic data for the paper. These data can be obtained free of charge at www.ccdc.cam.ac.uk/conts/retrieving.html [or from the Cambridge Crystallographic Data Center, 12, Union Road, Cambridge CB2 1EZ, UK; fax: (internet.) +44-1223/336-033; E-mail: deposit@ccdc.cam.ac.uk].

Acknowledgments

The project was sponsored by the Natural Science Foundation of Jiangsu Province (No. BK2009262). MO thanks the Grant-In-Aid for Science Research in a Priority Area 'Coordination Programming (No. 22108512)' and the Grant-In-Aid for Scientific Research Program (No. 23245014).

References

[1] (a) D. Tanaka, M. Higuchi, S. Horike, R. Matsuda, Y. Kinoshita, N. Yanai, S. Kitagawa, Chem. Asian J. 3 (2008) 1343–1349;
(b) L.J. Murray, M. Dinca, J.R. Long, Chem. Soc. Rev. 38 (2009) 1294–1314;
(c) S. Kitagawa, R. Kitaura, S. Noro, Angew. Chem. Int. Ed. 43 (2004) 2334–2375.
[2] (a) J.-L. Li, R.J. Kuppler, H.-C. Zhou, Chem. Soc. Rev. 38 (2009) 1477–1504;
(b) B.L. Chen, S.C. Xiang, G.D. Qian, Acc. Chem. Res. 43 (2010) 1115–1124.
[3] (a) M. Kurmoo, Chem. Soc. Rev. 38 (2009) 1353–1379;
(b) D. Maspoch, S.R. Molina, J. Veciana, Chem. Soc. Rev. 36 (2007) 770–818;
(c) N. Yanai, W. Kaneko, K. Yoneda, M. Ohba, S. Kitagawa, J. Am. Chem. Soc. 129 (2007) 3496–3497.
[4] (a) P. Horcajada, T. Chalati, C. Serre, B. Gillet, C. Sebrie, T. Baati, J.F. Eubank, D. Heurtaux, P. Clayette, C. Kreuz, J.-S. Chang, Y.K. Hwang, V. Marsaud, P.-N. Bories, L. Cynober, S. Gil, G. Ferey, P. Couvreur, R. Gref, Nat. Mater. 9 (2010) 172–178;
(b) K.M.L. Taylor-Pashow, J.D. Rocca, Z. Xie, S. Tran, W. Lin, J. Am. Chem. Soc. 131 (2009) 14261–14263.
[5] (a) L. Ma, C. Abney, W. Lin, Chem. Soc. Rev. 38 (2009) 1248–1256;
(b) J. Lee, O.K. Farha, J. Roberts, K.A. Scheidt, S.T. Nguyen, J.T. Hupp, Chem. Soc. Rev. 38 (2009) 1450–1459.
[6] (a) R. Ohtani, K. Yoneda, S. Furukawa, N. Horike, S. Kitagawa, A.B. Gaspar, M.C. Muñoz, J.A. Real, M. Ohba, J. Am. Chem. Soc. 133 (2011) 8600–8605;
(b) M. Ohba, K. Yoneda, G. Agusti, M.C. Muñoz, A.B. Gaspar, J.A. Real, M. Yamasaki, H. Ando, Y. Nakao, S. Sakaki, S. Kitagawa, Angew. Chem. Int. Ed. 48 (2009) 4767–4771;
(c) B.L. Chen, L.B. Wang, Y.Q. Xiao, F.R. Fronczek, M. Xue, Y.J. Cui, G.D. Qian, Angew. Chem. Int. Ed. 48 (2009) 500–503;
(d) A.J. Lan, K.H. Li, H.H. Wu, D.H. Olson, T.J. Emge, W. Ki, M.C. Hong, J. Li, Angew. Chem. Int. Ed. 48 (2009) 2334–2338;
(e) Z. Xie, L. Ma, K.E. deKrafft, A. Jin, W. Lin, J. Am. Chem. Soc. 132 (2010) 922–923.
[7] C.N.R. Rao, S. Natarajan, R. Vaidhyanathan, Angew. Chem. Int. Ed. 43 (2004) 1466–1496.
[8] (a) J. Chen, M. Ohba, D. Zhao, W. Kaneko, S. Kitagawa, Cryst. Growth Des. 6 (2006) 664–668;
(b) J. Chen, Z. Chen, T. Yu, L. Weng, B. Tu, D. Zhao, Micropor. Mesopor. Mater. 98 (2007) 16–20;
(c) A. Comotti, S. Bracco, P. Sozzani, S. Horike, R. Matsuda, J. Chen, M. Takata, Y. Kubota, S. Kitagawa, J. Am. Chem. Soc. 130 (2008) 13664–13672;
(d) J. Chen, S. Kitagawa, Chem. Lett. 39 (2010) 1186–1187;
(e) J. Chen, S. Kitagawa, Chem. Lett. 40 (2011) 656–657.
[9] A.K. Cheetham, C.N.R. Rao, R.K. Feller, Chem. Commun. (2006) 4780–4795.
[10] A.L. Spek, PLATON 99, A Multipurpose Crystallographic Tool, Utrecht University, Utrecht, The Netherlands, 1999.